Investigation of a Proposed ANN-Based Array Antenna Diagnosis Technique on a Planar Microstrip Array Antenna

A. R. Mallahzadeh and M. Taherzadeh

Faculty of Engineering, Shahed University, Tehran, Iran
mallahzadeh@shahed.ac.ir, taherzade@shahed.ac.ir

Abstract ─ In this article, a realistic neural network based method is proposed for the array antenna fault diagnosis through the utilization of array far field characteristics. Defective elements are those elements that are not excited directly by the feed lines but radiations due to the induced currents on the surface of these elements still remain. Neural network performs a nonlinear mapping between some samples of the degraded patterns and the array elements which may have caused these degradations. The proposed method is investigated on a real fabricated micro-strip planar array via its far field degraded radiation pattern measurements. A multilayer perceptron neural network trained in the back propagation mode with some samples of the simulated degraded patterns is used in an innovative manner to map the measured radiation pattern to its corresponding faulty elements configuration. After the training procedure the proposed fault diagnosis system is very fast and has a satisfactory success rate both in theory and application that makes it suitable for real time applications.

Index Terms ─ Array antenna, fault diagnosis, neural networks.

I. INTRODUCTION

The utilization abundance of large array antennas in a wide variety of applications particularly in spatial platforms proves the necessity of the elements performance monitoring and diagnosis systems on the array antennas of these applications. Array antenna elements fault diagnosis and compensation methods have been attended by many researchers in recent years. Element failure in array antenna may arise due to the disturbance in the driving equipments, feed lines, or array elements themselves which may result in elements radiation complete or partial failures. Element failure in a symmetric array causes it to be an asymmetrical array. It can distort the directivity of the antenna power pattern and it also leaves undesired effects on the side lobe level of the radiation pattern, voltage standing wave ratio and as a whole the good performance of the array antenna. Array antennas have this capability that with rearrangement in array elements excitations, the radiation pattern of antenna could be reconstructed to an acceptable pattern with minimum drops. In order to employ compensation methods, there should be an accurate locating of failure elements. Therefore, a major stage in the compensation procedure would be the failure elements locating. Employing the built in monitoring and calibration systems including a network of sensors is a very effective method in detecting faulty elements of arrays but it can enforce the probability of calibration system failures and an extended increase in volume, cost and design complexities on the system. Thus, the importance of the smart solutions can be realized.

One of the lately discussed smart solutions for this problem is the diagnosis of array antenna faults by the utilization of its far field information. This information consists of degraded radiation patterns that are measured from the base stations in definite spatial directions. Most of the array antenna fault detection methods employ the far field radiation patterns amplitudes that enhance the efficiency of method execution for the real time applications. In comparison with the array antenna built in fault isolation and correction systems [1], smart methods may not seem pragmatic. However with the exploitation of a fully projected far field

Submitted On: December 24, 2010
Accepted On: August 10, 2011

measurement and a robust diagnosis algorithm, smart fault diagnosis and compensation systems endorse an unmistakable detection of the failure elements area.

In fact, all of the array antenna fault diagnosis methods pursue the same policy. All methods are based on two major points. One point is the matter of handling a mathematical or geometrical model for the array antenna radiation patterns. Another point deals with the selection of an optimization or pattern recognition algorithm for minimizing the spacing between the degraded measured pattern and the predefined ones to investigate the failure elements configuration corresponding to the degraded pattern.

A genetic algorithm based method for detecting the number, location, and amount of failure in an 8×8 planar array was reported in [2]. In that report, a genetic algorithm was used to minimize a cost function that is the square of the difference between the power pattern of a given configuration of failed elements and the measured one. In [3], the element failure diagnosis of a planar array from its noisy far field power pattern was approached by the use of a genetic algorithm to reach an unambiguous solution of the problem. In [4], a reasonable method based on the array antenna simulation results was proposed for locating failure elements of a linear array from some samples of its simulated degraded patterns by the use of a MLP neural network. In that a defective element was considered as a non-radiating element but the mutual coupling effect between elements was considered. In [5], a support vector machine classifier was proposed to detect the failure elements of a linear array using different SVMs for different configuration of failed and perfect elements. In [6], the neural network was proposed for the diagnosis of phase and magnitude of current faults and the location of defective elements in a linear array from its degraded array factor. A case based reasoning algorithm was reported in [7] that resulted in an effective reduction in the search space of the genetic algorithm for fault detecting in a linear array.

Lately, optimization algorithms such as genetic algorithms proved themselves as the most reliable approach in array antenna fault diagnosis methods. In these methods, the genetic algorithm compares the degraded pattern with predefined patterns resulted from different chromosomes [8]. In this method, the genetic algorithm will be run for several times till the cost function reaches its optimized value. Then, the corresponding chromosome will represent the combination of faulty elements in an array antenna. However, the time needed for approaching the optimal cost function of genetic algorithm is a considerable disadvantage of the genetic algorithm based methods. Other pattern recognition tools such as neural networks and support vector machine aren't easy enough for implementing in large arrays [9]. In terms of the support vector machine it is necessary to define a different SVM for each array element to show which one is perfect and which one is faulty or for each combination of array element failures. Despite complications of these methods, a well-trained MLP or SVM could be very useful in real time applications due to their fast responding time.

As former studies, in the present study element failure diagnosis is performed by the use of array antennas far field characteristics. Here, the defective element is not considered as a non-radiating element with no output and the radiation due to the induced currents is considered as well as the mutual coupling effect.

II. THE METHOD

The implementation of fault detection and compensation methods together with one of the beam forming techniques makes a simple continuous monitoring on the array antenna elements performance and at a higher level of proposition it also equips the array antenna radiation pattern with an instantaneous closed loop control.

A bunch of complexities in setting up stage of the array diagnosis techniques comes about radiation patterns representation. Some of the already proposed methods have utilized the array factor and element factor for attaining this purpose [2, 3, 6] and some others have made use of simulated patterns to establish a look up table of the array antenna probable radiation patterns [4]. All of the aforementioned methods can be classified into two categories: In the first category are those methods that have radiation pattern calculations in them and are based on the array factor calculation. Evidently in these works, the mutual coupling effect has been neglected. In the

second category are those methods that are based on the simulation results of antennas. However in these works, the mutual coupling effect is considered, the radiation of the defective elements in front of other normal elements has been neglected. But in practice a defective antenna element could be a radiating one itself via its surface induced currents resulted from the radiation fields of the normal elements. Thus, the removal of defective elements is equal to the elimination of this radiation portion and may reduce reliability and success rate of the fault diagnosis systems.

The proposed method in this work is a neural network based approach that exercises the simulated radiation patterns of a fully simulated planar array antenna including feed lines. Preparation of the fault diagnosis procedure initiates with simulating the entire possible cases of the array elements failure configurations. Simulated pattern samples from certain spatial directions as well as the corresponding configurations of the faulty element numbers and locations raise input and target vectors of a MLP artificial neural network. The proposed neural network has been trained with radiation pattern samples of simulated array antenna and tested with measured radiation pattern samples of the fabricated antenna.

The preference of the neural networks in the suggested method is a comparative selection. In some aspects, neural network is the best optimum choice and in some others it is just a mediocre selection. As a result of the wide diversity of the optimization, classification, and pattern recognition algorithms, there are a large number of options for the array antenna diagnosis objectives. These options winning depend on the problem, its applications, and particularly time limitations. The utilization of neural network in this paper in addition to effectiveness is performed due to its intrinsic fast responding time that makes it appropriate for in time applications. So it can easily be implemented on some programmed hardware for using an online array antenna pattern measurements and fault detections.

The proposed method is tested on a typical fabricated array antenna and after some post-processing procedures has a satisfactory success rate both in theory and application.

III. STATEMENT OF THE PROBLEM

Here, the goal is to investigate the proposed approach on a typical micro-strip planar array antenna. The proposed antenna is just an example and the method can be extended to any type of arrays. The designated array antenna is a 4×4 uniformly excited micro-strip planar array antenna with $228.35\ mil \times 228.35\ mil$ square patches that are spaced 0.69λ from each other at the frequency of 16.2GHz. The antenna structure is designed and fabricated on a Rogers RT/duroid 5880 substrate of 20mil thickness and dielectric constant of 2.2. microstrip antenna is fed by a 50Ω coaxial cable through a standard SMA connector. The simulated array structure is shown in Fig. 1. Antenna array simulations are made by the use of HFSS11.

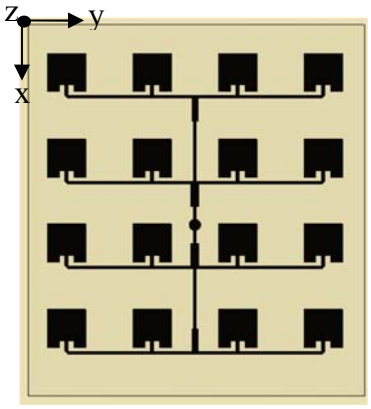

Fig. 1. 4×4 micro-strip planar array antenna.

The antenna performance is monitored at the frequency range of 16.2GHz to 16.8GHz at 200MHz steps. Application of the method is studied in these 4 frequencies. The corresponding antenna VSWRs and gains at the above frequency range are presented in Fig. 2 and Fig. 3.

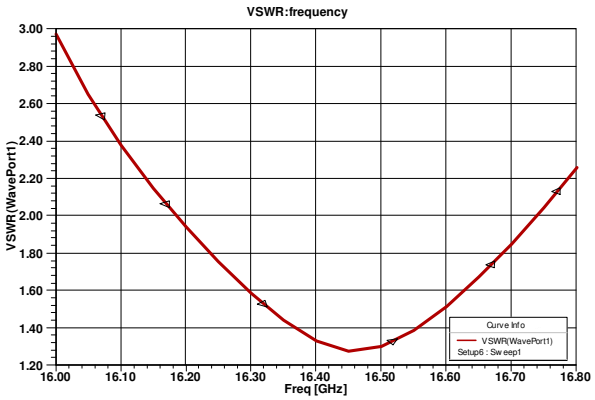

Fig. 2. VSWR of the array antenna of Fig. 1.

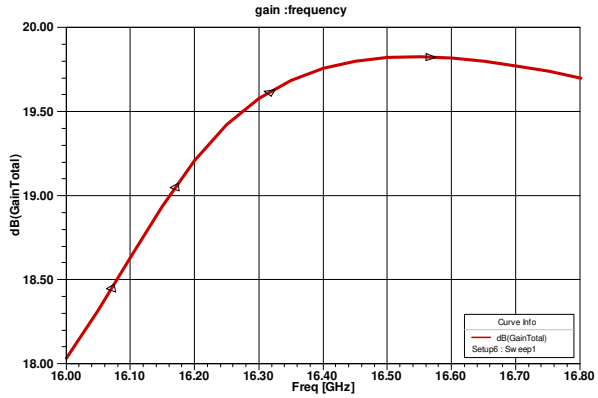

Fig. 3. Gain of the array antenna of Fig. 1.

Some cases of deviated antenna patterns have been shown in Fig. 4a and Fig. 4b in $\phi = 0°$ and $\phi = 90°$ principle planes and at the design frequency of 16.2GHz.

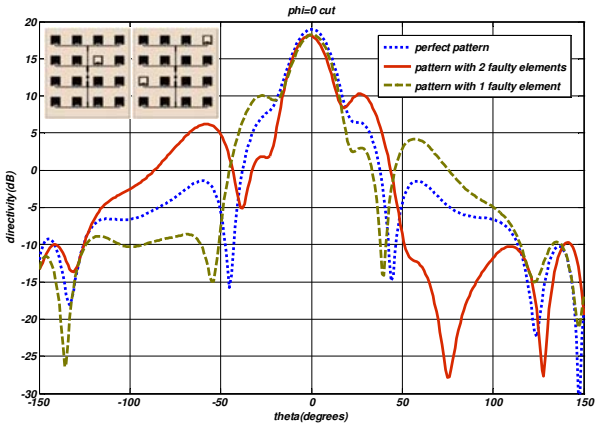

(a)

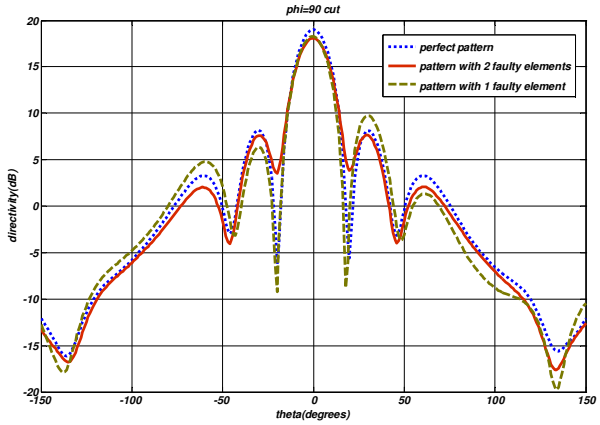

(b)

Fig. 4. Radiation pattern of the array antenna of Figure 1 for some typical cases of failure for 1 and 2 faulty elements in principle planes of (a) $\phi = 0°$ and (b) $\phi = 90°$.

These deviations are due to the failure of some randomly chosen elements of the array including one defective element and two defective elements in comparison with an antenna without any failed element. It can be observed from Fig. 4a and Fig. 4b that element failure in this particular antenna has its most deviating effects on phi=0 cuts of radiation patterns.

For examination of the failure diagnosis system on the abovementioned array antenna, some assumptions have been made to simplify the procedure:

- The probability of malfunctioning in more than two elements of a 16 elements array antenna is so unlikely;
- Defective elements are supposed as the elements that are not excited by the feed lines directly;
- Some cases of element failures have no significant destructive influence on the antenna radiation pattern. These cases are treated as don't care cases.

The radiation patterns of one of the don't care cases have been shown in Fig. 5- Fig. 8 in principle planes of $\phi = 0°$ at the aforementioned frequencies. It can be seen from these figures that in that specified case element failure effects are negligible and they don't include any serious damage on antenna radiation patterns even for different cuts. Thus, inclusion of these cases in the diagnosis procedure and detecting of these kinds of failures doesn't have any helpful information for compensation algorithms and it only increases fault locating complexities and misjudging of the method implementation.

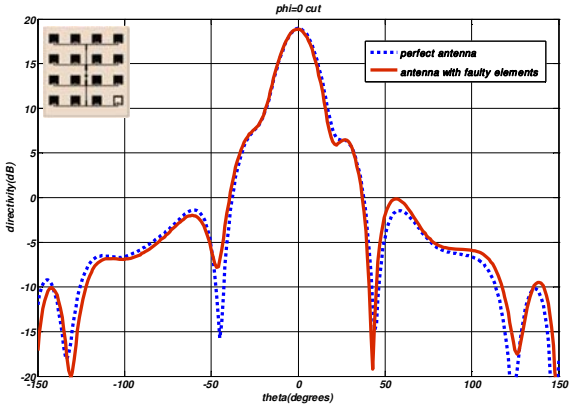

Fig. 5. An example of don't care cases in principle plane of phi=0 at 16.2GHz.

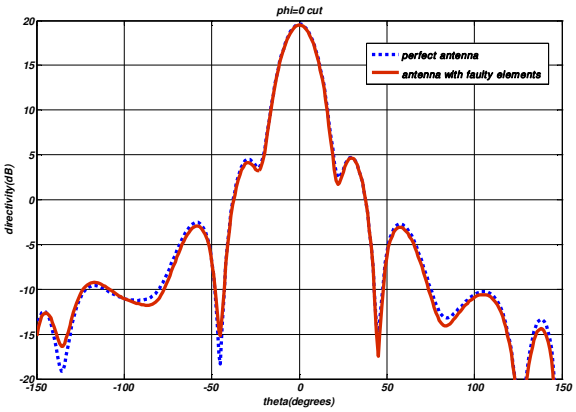

Fig. 6. An example of don't care cases in principle plane of phi=0 at 16.4GHz.

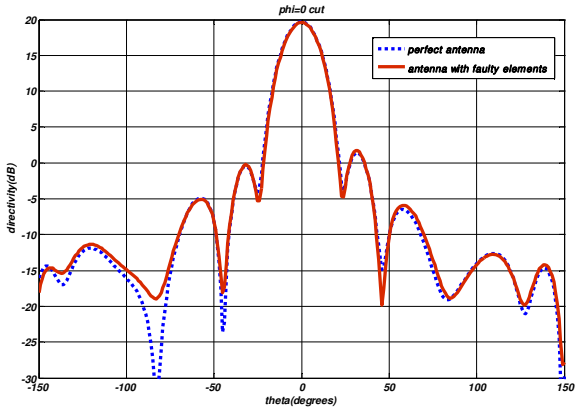

Fig. 7. An example of don't care cases in principle plane of phi=0 at 16.6GHz.

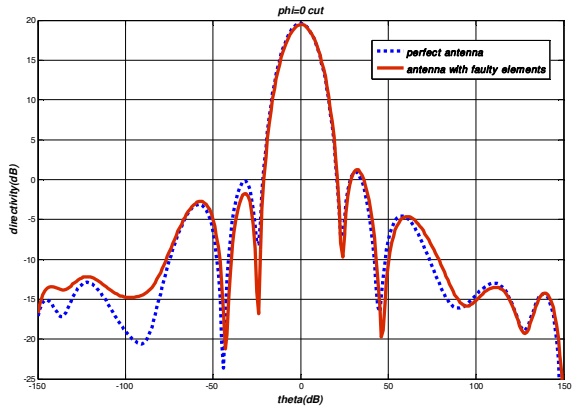

Fig. 8. An example of don't care cases in principle plane of phi=0 at 16.8GHz.

The assumed type of fault in this paper is equivalent to the elements zero excitation in the preceding articles. Although this type of fault generating may seem restrictive, it is appropriate for the aim of considering the parasitic presence of the malfunctioning elements in the array structure. Besides this type of fault forming, covers some special kind of array antenna faults could be named as elements feed line failure.

IV. THE NEURAL NETWORK

MLP neural networks are generally multilayer feed forward neural networks that apply two kinds of differentiable signals: functional signals and error signals. Functional signals move forward through the neurons and error signals move backward. Each of the neurons operates both the functional signal and the error gradient approximation. A neural network with sigmoid transfer function in the hidden layer and linear transfer function in the output layer would be able to approximate any nonlinear function [10].

In this study, a three layers MLP neural network is trained in the back propagation learning mode that uses the gradient decent optimization methods in the learning procedure, for readjusting the weights of the network from the below formula [11]:

$$w_{ij}(t+1) = w_{ij}(t) - \eta \frac{\partial E}{\partial w_{ij}}, \qquad (1)$$

where η is a constant called learning rate, w is the connecting weight and E is the mean square error in the output layer. It is possible to use the *msereg* regularized performance function for error calculation that is appropriate for the training procedure of large training sets. This performance function could be defined by this formula:

$$msereg = \gamma \frac{1}{N}\sum_{i=1}^{N}(t_i\text{-}a_i)^2 + (1-\gamma)\frac{1}{n}\sum_{j=1}^{n} w_j^2, \qquad (2)$$

where γ, the performance ratio, is a user selected constant, N is the number of output layer neurons, and n is the total number of the network weights and biases. This regularized performance function enforces the network to have smoother weights and biases and avoids the neural network answers from unexpected changes. The block diagram of a three layers MLP neural network is shown in Fig. 9 which L, M, and N, respectively are total number of neurons in input layer, hidden layer,

and output layer. **p** is the input vector and **a** is the network output which can be obtained by the use of weights, biases, and transfer functions of each layer.

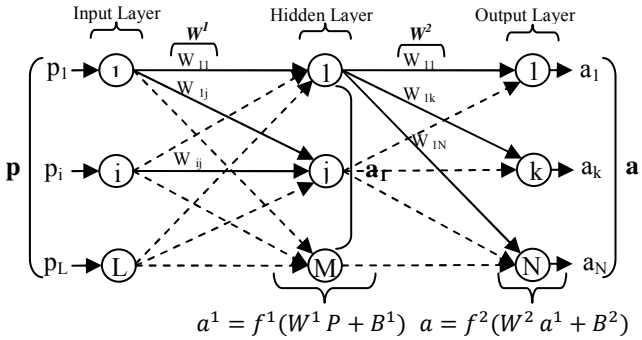

Fig. 9. Block diagram of a typical three layers MLP neural network.

V. METHOD IMPLEMENTATION

The total number of simulated patterns for each frequency is 137 which consists of antenna array cases with 2 failure elements, $\binom{16}{2}$, cases with 1 failure element, 16, and the case in which all array elements are working properly. The most deviations due to the antenna elements failure has been observed in $\phi = 0°$ principle planes of the radiation patterns. Hence, the neural network input vector has been managed by some samples of this principle plane which also encompasses adequate information needed for fault area detection. It could be observed from the simulated directivity patterns of Fig. 10- Fig. 13 that element failure causes sharp destructive variations such as gain drop, SLL increasing and directivity losing on the antenna far field radiation pattern. The defective elements of the array are declared with white marked elements at the abovementioned figures. Failure is resulted from interrupting the adjacent feed lines of some certain elements. Each figure demonstrates two radiation patterns for each frequency: one for perfect radiations of antenna elements and another for degradation in some antenna elements.

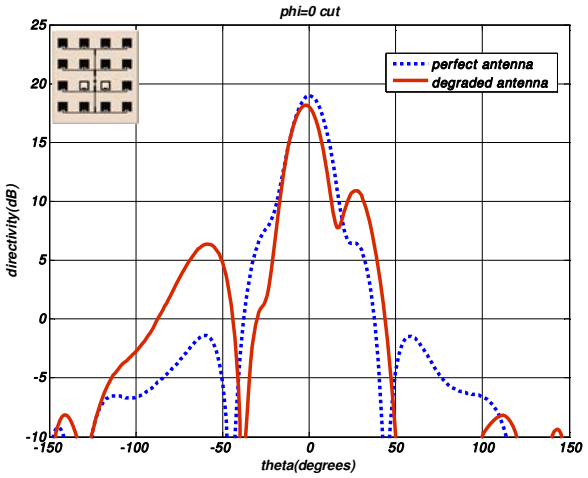

Fig. 10. H-plane directivity patterns of 4×4 array for perfect and degraded antenna at 16.2GHz.

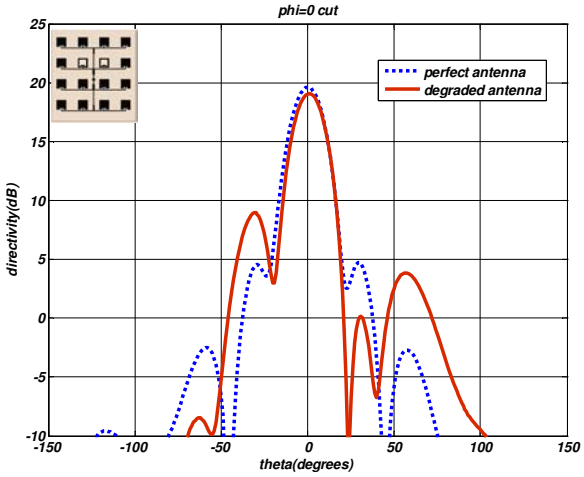

Fig. 11. H-plane directivity patterns of 4×4 array for perfect and degraded antenna at 16.4GHz.

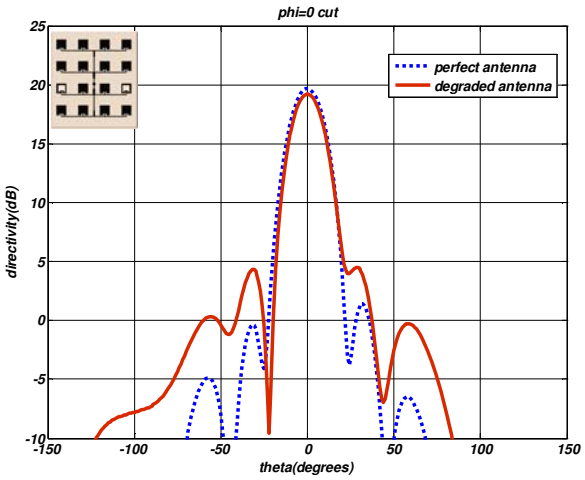

Fig. 12. H-plane directivity patterns of 4×4 array for perfect and degraded antenna at 16.6GHz.

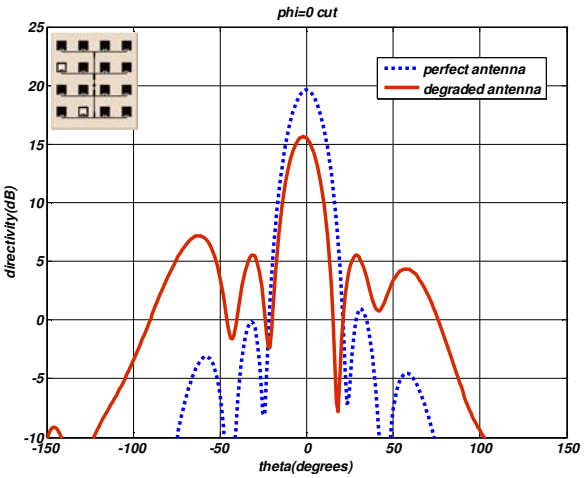

Fig. 13. H-plane directivity patterns of 4×4 array for perfect and degraded antenna at 16.8GHz.

A. Antenna fabrication

Here, the practicability of the suggested method has been examined through the array diagnosis procedure realization on a fabricated antenna. Figure 14 represents the fabricated antenna of Fig. 1. First, the antenna output has been measured with all array elements in perfect radiation condition. The related radiation patterns can be observed from Fig. 15 to Fig. 18 that are all normalized to take their maximum amplitude at 0dB. As it could be seen, there is a good agreement between the simulated radiation patterns and the measured ones.

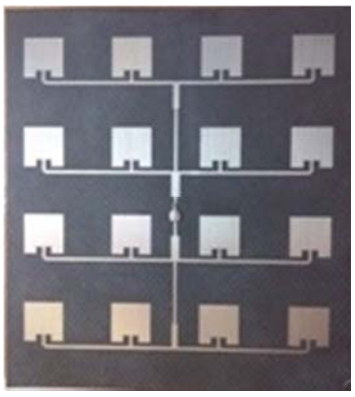

Fig. 14. Fabricated microstrip array antenna.

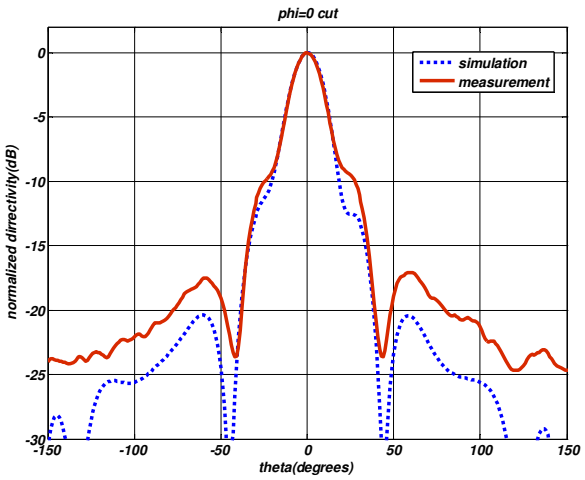

Fig. 15. Simulated and measured H-plane radiation patterns of perfect antenna at 16.2GHz.

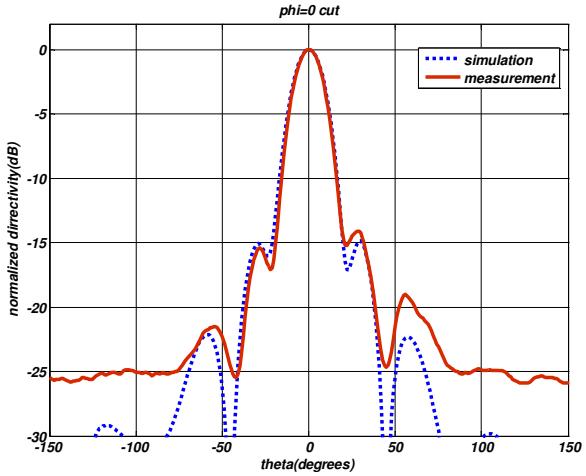

Fig. 16. Simulated and measured H-plane radiation patterns of perfect antenna at 16.4GHz.

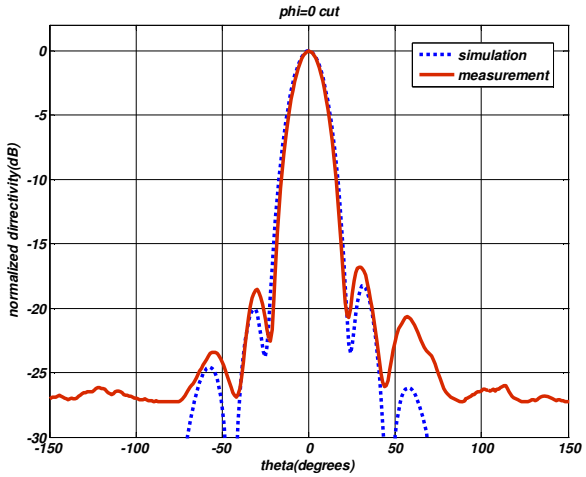

Fig. 17. Simulated and measured H-plane radiation patterns of perfect antenna at 16.6GHz.

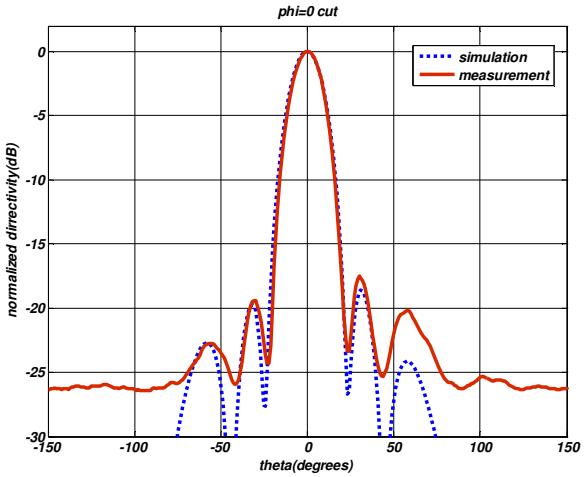

Fig. 18. Simulated and measured H-plane radiation patterns of perfect antenna at 16.8GHz.

B. Fault generation on the fabricated antenna

To create failure in a radiation pattern, one of the possible fault configurations has been implemented on the fabricated antenna. In this stage, the adjacent feed lines of two randomly chosen elements has been broken down in such a way that elements became completely out of direct excitation. The corresponding measured radiation patterns are illustrated in Fig. 19 to Fig. 22 that are also normalized to take maximum amplitude of 0dB. The failure elements could be seen as white marked elements in Fig. 19.

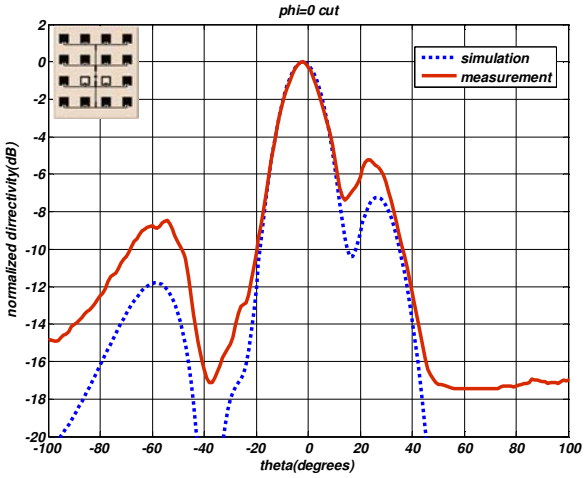

Fig. 19. Simulated and measured H-plane radiation patterns of degraded antenna at 16.2GHz.

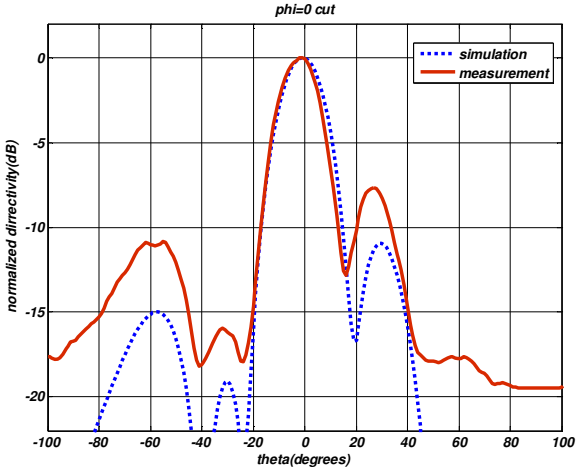

Fig. 20. Simulated and measured H-plane radiation patterns of degraded antenna at 16.4GHz.

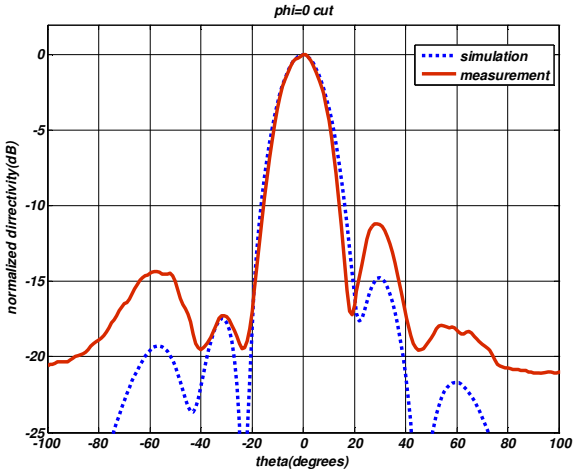

Fig. 21. Simulated and measured H-plane radiation patterns of degraded antenna at 16.6GHz.

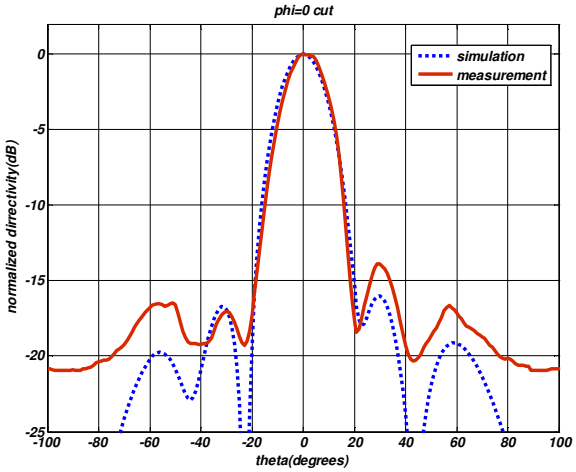

Fig. 22. Simulated and measured H-plane radiation patterns of degraded antenna at 16.8GHz.

C. Patterns sampling and ANN training

It could be observed from Fig. 15 to Fig. 22 that in comparison with the simulation results considerable mismatching in the measurement results comes about elevation angles beyond the $\boldsymbol{\theta} = [-\mathbf{50}^\circ, \mathbf{50}^\circ]$. So to construct the neural network input vectors the radiation patterns are sampled in this specific range. Besides all required specifications of the radiation patterns such as main lobe amplitude and side lobes level could be elicited easily from this sampling range.

As a result of array symmetry and elements bordering there are a lot of fault cases that radiation patterns of them have no conspicuous difference from each other. These cases mostly happen in two sides of antenna X direction symmetry axis due to the exact same geometrical shape of these two halves. To simplify the procedure, from the entire simulated patterns of each frequency, 54 fault cases could be removed including both the repeated cases and don't care cases. All other 83 failure cases have been employed for neural network training and fault diagnosis process.

Here, the neural network is a three layer MLP neural network with a sigmoid transfer function in the hidden layer and a linear transfer function in the output layer. The number of input neurons is equal to the number of radiation patterns samples. The neural network has been initialized for the learning procedure with two different input vectors: one with 5 degree steps and another with 1 degree steps sampling along the simulated radiation patterns. The number of output layer neurons is equal to the maximum number of array defective elements which in the assumed problem is two elements. The number of hidden layer neurons depends on the problem circumstances. In this work, the number of hidden layer neurons has been chosen 100 neurons. The procedure followed to select the proper value for hidden layer neurons consists of two test sets: one the same as train set input vector and another with 0.2dB error from the train set. It has been explored from several training and testing procedures that the network with less than 100 neurons in hidden layer didn't reach the goal of 100% failure detection even for testing its own train sets. On the other hand, the network with more than 100 neurons in a hidden layer didn't seem reliable enough for fault detection of cases with 0.5dB error at the desired accuracy. So 100 have been preferred as optimal value for the number of hidden layer neurons of MLP neural network in this work. Table 1 shows the neural network training parameters.

Preprocessing of the neural network inputs comprises a normalization procedure that results in smoother variations in the input vectors of the MLP neural network. The neural network training input vector is some samples of all simulated degraded patterns plus one perfect radiation pattern. Output vector consists of two neurons that are labeled with two numbers from 1 to 16 corresponded to the failed elements location from the left top of the array antenna in Fig. 1 and an all zero column corresponded to the perfect radiation .

Table 1: MLP neural network training parameters for 2 different sampling steps

Sampling step ($\boldsymbol{\theta}^\circ$)	5	1
Input layer neurons	21	101
Hidden layer neurons	100	100
Output layer neurons	2	2
Transfer function	msereg	msereg
Performance function goal	1×10^{-8}	1×10^{-8}
Performance ratio	0.99	0.99
Learning rate	0.05	0.05
Training time (min)	10-12	20-25

D. Fault exploitation using the trained MLP neural network

The trained MLP has been tested by the fabricated faults. Radiation patterns of the fabricated degraded antenna at $\phi = 0^\circ$ principle planes have been normalized to a normalization factor that has been obtained from the average of the neural network input vectors. The normalized pattern has been sampled in elevation angles of $[-50^\circ, 50^\circ]$ in two sampling sets of 21 samples and 101 samples.

Exploitation of an antenna failure situation from the response of the neural network could be performed through the defining of some element failure vicinities. In the other word, the surface of the array antenna could be imagined as a 16 blocks continues radiating surface in which one block malfunctioning may result in closely the same degradations as the adjoining block does. For each failing element candidate, this vicinity has two boundaries defined as $X \pm 0.5$ where X is an integer value from 1 to 16 corresponding to the

elements number. The neural network response deviation rate can be adjusted via the obtained results distances from these boundaries. Because of the elements symmetry in the most general array structures, Utilization of the neural network may result in several answers. For example, if the neural network responses are 7.45 and 12.7 it means that all elements of 7, 8, 12, and 13 have some chances to be the failed element. Thus, the deviation of network responses from the boundaries of these element numbers $(X \pm 0.5)$ determines the failure happening probability of each of these elements. In this example, the boundaries of elements 7 and 8 are respectively [6.5, 7.5] and [7.5, 8.5]. So according to the neural network response, the failure happening probabilities of elements 7 and 8 are, respectively, 100% and 95%. The best preferred answer would be the one that has minimum departures from some specified response vicinity.

VI. RESULTS AND DISCUSSIONS

The results of the trained MLP neural network in response to the degraded pattern of fabricated antenna showed satisfactory success rates. These results for two trained MLPs have been illustrated in Table 2 and Table 3. There are three collections of answers that are arranged based on the occurrence probability. Answer collections 1 to 3 include the responses with, respectively, 100%, above 80% and between 20% and 80% happening probabilities.

The corresponding success rates of the trained MLP results could be observed from Fig. 23 and Fig. 24 which show the accomplishment of the method in detecting the area of the fabricated failures. The ideal answers would be 10 and 11 resulted from fault locations illustrated in Fig. 19 with white marked elements. Success rates illustrated in Fig. 23 and Fig. 24 determine the closeness percents of 1st answer sets to the desired answers that are [9.5, 10.5] and [10.5, 11.5], respectively, for elements 10 and 11. As a result of array elements bordering it should be mentioned that answers with success rates of less than 100% are also in the matter of consideration. This means that all of the fault diagnosis procedures need to be accompanied with one of the compensation methods and a second measurement to assure the correctness of the detected failures. The procedure needed for exploring other cases of faults such as 1 or 2 other elements failure from the trained MLP is the same. This method in corporation with a reliable measurement can be applied on any type of linear or planar arrays and it also can be programmed on some hardware such as FPGA for real time applications.

VII. CONCLUSION

A fault detection method was proposed for planar array antenna elements diagnosis based on some samples of their degraded radiation patterns. A MLP neural network was trained for mapping the degraded radiation patterns to the corresponding configurations of array elements failure. The proposed method was implemented on a fabricated 4×4 micro-strip planar array antenna degraded with interrupting the feed lines of some

Table 2: Test results of the MLP neural network trained with radiation patterns 21 samples

Frequency (GHz)	MLP neural network outputs		1st answer set		2nd answer set		3rd answer set	
16.2	12.5	10.7	12	11	13	10	---	12
16.4	11.7	9.54	12	10	11	9	---	---
16.6	11.7	9.89	12	10	11	---	---	9
16.8	12.2	9.45	12	9	---	10	11	---

Table 3: Test results of the MLP neural network trained with radiation patterns 101 samples

Frequency (GHz)	MLP neural network outputs		1st answer set		2nd answer set		3rd answer set	
16.2	10.01	10.56	10	11	---	10	11	---
16.4	10.62	10.8	11	11	10	10	---	---
16.6	11.14	9.67	11	10	---	9	12	---
16.8	10.83	9.34	11	9	---	10	10	---

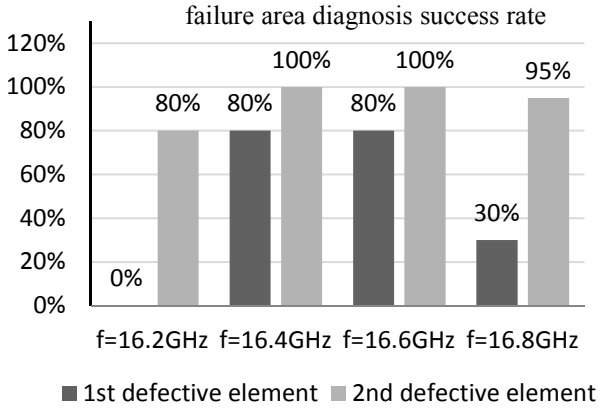

Fig. 23. Fault location diagnosis success rates of MLP neural network trained with 21 samples at 4 frequencies.

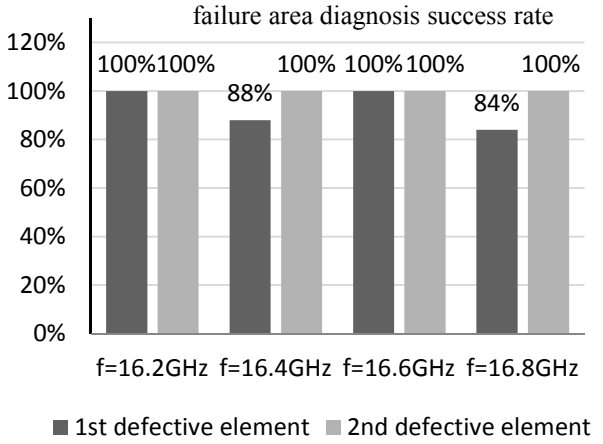

Fig. 24. Fault location diagnosis success rate of MLP neural network trained with 101 samples at 4 frequencies.

randomly chosen elements. The MLP neural network outputs showed a fast and successful achievement of method to the fault happening areas. The major difference between this work and the preceding works is in the consideration of mutual coupling effects as well as the radiated field of the so called faulty element.

REFERENCES

[1] K. M. Lee, R. S. Chu, and S. C. Liu, "A Built-In Performance-Monitoring/Fault Isolation and Correction (PM/FIC) System for Active Phased-Array Antennas," IEEE Transactions on Antennas and Propagation, vol. 41, no. 11, pp. 1530-1540, November 1993.

[2] J. A. Rodríguez, F. Ares, H. Palacios, and J. Vassal'lo, "Finding Defective Elements in Planar Arrays Using Genetic Algorithms," *Progress In Electromagnetics Research*, *PIER*, vol. 29, pp. 25-37, 2000.

[3] O. M. Bucci, A. Capozzoli, and G. D'Elia, "Diagnosis of Array Faults from Far-Field Amplitude-Only Data," IEEE Transactions on Antennas and Propagation, vol. 48, no. 5, pp. 647-652, May 2000.

[4] A. Patnaik, B. Choudhury, P. Pradhan, R. K. Mishra, and C. Christodoulou, "An ANN Application for Fault Finding in Antenna Arrays," IEEE Transactions on Antennas and Propagation, vol. 55, no. 3, pp. 775-777, March 2007.

[5] N. Xu, C. G. Christodoulou, S. E. Barbin, and M. Martínez-Ramón, "Detecting Failure of Antenna Array Elements Using Machine Learning Optimization," IEEE International Symposium on Antennas and Propagation, pp. 5753-5756, June 2007.

[6] N. V. S. N. Sarma and D. Vakula, "A Method for Diagnosis of Current Faults in Antenna Arrays Using Neural Networks," International Journal of RF and Microwave Computer-Aided Engineering, 2008.

[7] R. Iglesias, F.Ares, M. Fernández-Delgado, J. A. Rodríguez, J. Brégains, and S. Barro, "Element Failure Detection in Linear Antenna Arrays Using Case-Based Reasoning," IEEE Antennas and Propagation Magazine, vol. 50, no. 4, pp.198-204, August 2008.

[8] R. L. Haupt, "Introduction to Genetic Algorithms in Electromagnetics," Applied Computational Electromagnetic Society (ACES) Journal, vol.15, no. 2, 2000.

[9] R. Ghayoula, N. Fadlallah, A. Gharsallah, and M. Rammal, "Design, Modelling, and Synthesis of Radiation Pattern of Intelligent Antenna by Artificial Neural Networks," Applied Computational Electromagnetic Society (ACES) Journal, vol. 23, no. 4, pp. 336–344, December 2008.

[10] S. Haykin, Neural networks A comprehensive foundation, Pearson Education, Inc, 2002.

[11] A. Patnaik and R. K. Mishra, "ANN Techniques in Microwave Engineering," IEEE Microwave Magazine, vol. 1, pp. 55-60, March 2000.

[12] J. D. Kraus and R. J. Marhefka, Antennas for All Applications. 3RD edition, McGraw-Hill Science Engineering, 2001.

Alireza Mallahzadeh received the B.S. degree in Electrical Engineering from Isfahan University of Technology, Isfahan, Iran, in 1999 and M.S. degree in Electrical Engineering from Iran University of Science and Technology, Tehran, in 2001, and the Ph.D. degree in Electrical Engineering from Iran University of Science and Technology, Tehran, in 2006. He is a member of the academic staff, Faculty of Engineering, Shahed University, Tehran. He has participated in many projects relative to antenna design, which resulted in fabricating different types of antennas for various companies. Also, he is interested in numerical modeling, and microwaves.

Motahareh Taherzadeh received the B.S. in Electrical Engineering from Semnan University, Semnen, Iran, in 2006 and the M.S. in Electrical Engineering from Shahed University, Tehran, Iran, in 2010. Her research interests include array antennas fault diagnosis techniques, optimization and pattern recognition methods and software development for smart solving of electromagnetic problems.